



Title	A lipid nanoparticle for the efficient delivery of siRNA to dendritic cells
Author(s)	Warashina, Shota; Nakamura, Takashi; Sato, Yusuke; Fujiwara, Yuki; Hyodo, Mamoru; Hatakeyama, Hiroto; Harashima, Hideyoshi
Citation	Journal of controlled release, 225, 183-191 https://doi.org/10.1016/j.jconrel.2016.01.042
Issue Date	2016-03-10
Doc URL	http://hdl.handle.net/2115/64690
Rights	©2016 , Elsevier. This manuscript version is made available under the CC-BY-NC-ND 4.0 license http://creativecommons.org/licenses/by-nc-nd/4.0/
Rights(URL)	http://creativecommons.org/licenses/by-nc-nd/4.0/
Type	article (author version)
File Information	JCR 225. 183-191, 2016 HUSCAP.pdf



[Instructions for use](#)

Title

A lipid nanoparticle for the efficient delivery of siRNA to dendritic cells

Author

Shota Warashina^a, Takashi Nakamura^a, Yusuke Sato^a, Yuki Fujiwara^a, Mamoru Hyodo^b, Hiroto Hatakeyama^c, and Hideyoshi Harashima^{a*}

^aFaculty of Pharmaceutical Sciences, Hokkaido University, Kita-12, Nishi-6, Kita-ku, Sapporo 060-0812, Japan

^bDepartment of Applied Chemistry, Faculty of Engineering, Aichi Institute of Technology, 1247 Yachigusa, Yakusa-Cho, Toyota 470-0392, Japan

^cDepartment of Gynecologic Oncology and Reproductive Medicine, The University of Texas MD Anderson Cancer Center, 1515 Holcombe Blvd, Houston, TX 77030, USA

*Correspondence:

Hideyoshi Harashima, Faculty of Pharmaceutical Sciences, Hokkaido University, Sapporo, Hokkaido 060-0812, Japan.

Telephone: +81-11-706-3919, Fax: +81-11-706-3734

E-mail: harasima@pharm.hokudai.ac.jp

Abstract

Applying small interfering RNA (siRNA) to dendritic cell (DC) based therapy represents a potential candidate for cancer immunotherapy. However, delivering siRNA to DCs is a challenging issue for non-viral vectors. To date, only viral vectors have achieved efficient gene silencing in DCs. We report herein that a novel cationic lipid, YSK12-C4, when loaded in a nanoparticle with siRNA (YSK12-C4 multifunctional envelope type nano device [YSK12-MEND]), greatly facilitated gene silencing in mouse DCs. The use of the YSK12-MEND resulted in a gene silencing efficiency in excess of 90%, with a median effective dose (ED₅₀) of 1.5 nM, whereas the maximum gene silencing efficiency of Lipofectamine RNAi MAX was less than 60% and the EC₅₀ was 25 nM. Furthermore, a suppressor of cytokine signaling 1, an immune suppressive molecule in DCs, silenced in the mouse DC by the YSK12-MEND showed a drastic enhancement in cytokine production, resulting in the significant suppression of tumor growth when it was applied to DC-based therapy against a mouse lymphoma. These results clearly indicate that YSK12-MEND overcomes the obstacle associated with non-viral vectors and can be considered to be a promising non-viral vector for siRNA

delivery to DCs, thus accelerating DC-based therapies with siRNA.

KEYWORDS: cancer immunotherapy; siRNA nanoparticle; dendritic cell; endosomal escape; SOCS1; dendritic cell-based vaccine

1. Introduction

PROVENGE®, an autologous cell-based immunotherapy using activated blood mononuclear cells including dendritic cells (DCs), was first approved in 2010 by the US FDA for use in the treatment of prostate cancer. In addition, several clinical trials of DC-based therapy are currently underway [1]. In this review, clinical trials that are currently registered at www.clinicaltrials.gov are overviewed. However, the DC-based therapy has received a great deal of criticism, and even skepticism, because of the insufficient therapeutic effect in terms of inducing objective clinical responses [2]. On the other hand, Anguille et al., in a systemic review, reported that, of all the published clinical trials to document the proportion of patients who showed objective responses and overall survival, DC-based therapy drastically improved survival, although the clinical benefit in terms of classic objective tumor response is small [1]. They also advocated implementation of alternative endpoints to assess the true clinical potency of DC-based therapy. In addition, another advantageous benefit of DC-based therapy is safety and its low toxicity is expected to keep the quality of life of cancer patients. Therefore, DC-based therapy appears to be a well-tolerated immunotherapeutic method and will likely develop as one of the main stream therapies in the field of cancer immunotherapy in the future.

Although the criteria may be need to be altered in the case of cancer immunotherapy, the fact that the objective tumor response rates rarely exceeded 15% is clearly a problem [1]. To overcome this problem, the development of new types of DC-based therapies are underway: the use of DC products with an improved immunogenicity such as mature DCs producing IL12p70 and Langerhans cell-type DCs; the enhancement of DC-based therapy through combination with other drugs such as immune checkpoint inhibitors, adjuvants, cytokines and anti-cancer drugs [1]. In particular, the combination therapies are based on the strategies focused on enhancing the strength of immune responses, and breaking tumor-associated immunosuppression. Both strategies are being actively pursued in the area of cancer immunotherapy. However, the effects of mature DCs and Langerhans cells administered to cancer patients will decrease as the result of immunosuppression by tumors, even if they are improved the immunogenicity. Side-effects will be a concern in combination therapies with other drugs, resulting in the loss of safety of DC-based therapy. Therefore, it is necessary for DC itself to be equipped with a “sword” to improve its strength of immunity and a “shield” to prevent immunosuppression in a tumor microenvironment. To achieve this, DC functions need to be strictly controlled. The use of RNA interference (RNAi) represents a potent technique for controlling DC functions. RNAi

technology can selectively control the expression of target molecules, resulting in the strict control of DC functions. Gene silencing of negative-feedback factors in DCs, such as the suppressor of cytokine signaling 1 (SOCS1) and A20, would be expected to greatly stimulate cytokine production and antitumor activity [3,4]. In addition to improving the strength of immunity mediated by DCs, gene silencing of the transforming growth factor β (TGF- β) receptor in DCs can result in the prevention of tumor-associated immunosuppression, because DC functions are also suppressed by TGF- β in a tumor microenvironment [5]. The inhibition of the indoleamine-2,3 dioxygenase (IDO) enzyme in DCs also represents a promising strategy for the prevention of tumor-associated immunosuppression [6]. Therefore, the control of DC functions mediated by RNAi technology would be a potentially potent strategy for next-generation DC-based therapy.

However, gene silencing in DCs is quite difficult to achieve with conventional methodology [7]. Hence, in the above studies, a lentivirus vector expressing short hairpin RNA was used [3,4]. In the case of a clinical application, however, a non-viral approach can be more desirable than a viral vector, which have been reported to show serious side effects in clinical trials [8]. Some studies have demonstrated that DCs can be gene silenced using non-viral methods including commercially available transfection reagents such as LipofectamineTM 2000 [9-14]. The small interfering RNA (siRNA) doses used in these reported studies were 100 nM – 4 μ M in transfection to DCs, which was considerably higher than the dose used in transfection when other cell lines are used. We also demonstrated gene silencing in DCs using multifunctional envelope-type nano device (MEND), a number of our original non-viral vector series [15,16]. The MEND is a lipid-based nanoparticle and is designed for controlling intracellular trafficking in addition to tissue distribution by virtue of being modified with several functional molecules and varying lipid components [17,18]. The siRNA-loaded MEND, namely R8/GALA-MEND_{SUV}, was constructed by mixing an siRNA/stearylated octaarginine (siRNA/STR-R8) complex with small unilamellar vesicles (SUVs), and the lipid surfaces of preparation was modified with STR-R8 and the GALA peptide [15,16]. The R8 peptide, a type of cell-penetrating peptide, increases the cell affinity of MEND and GALA peptide has a pH-sensitive fusogenic activity for enhancing endosomal escape [19,20]. The R8/GALA-MEND_{SUV} induced strong gene silencing in HeLa cells at a siRNA dose of 12 nM [15]. Gene silencing of SOCS1 or A20 in DC was observed at a siRNA dose of 80 nM, whereas the efficiency of gene silencing was only modest (40-70%) [15,16]. On the other hand, a viral vector achieved more than 80% gene

silencing [3,4]. Based on these findings, it is clear that a breakthrough delivery system is needed for the efficient introduction of siRNA to DCs.

Here, we report on the development of YSK12-C4, a novel ionizable-cationic lipid, which breaks the barrier of siRNA delivery for DCs. The YSK12-C4 containing MEND loaded with siRNA (YSK12-MEND) has a high pKa (8.0). This high pKa can be an advantage for the efficient endosomal escape in DCs, because it has been reported that the acidification of endosomes containing antigens is a slow process [21,22]. In addition, we expected that the cellular uptake of siRNA would be enhanced at a neutral pH. Strikingly, the median effective dose (ED₅₀) for gene silencing by the YSK12-MEND was 1.5 nM, which was drastically lower than the doses of LipofectamineTM RNAiMAX (RNAiMAX) (ED₅₀ = 25 nM) and the R8/GALA-MEND_{SUV} (ED₅₀ = 70 nM). The YSK12-MEND also showed more than 80% gene silencing of SOCS1 at a siRNA dose of 3 nM. Moreover, immunization with SOCS1-silenced DC by the YSK12-MEND completely inhibited tumor growth in lymphoma bearing mice, compared with the resulted for RNAiMAX and R8/GALA-MEND_{SUV}. These findings clearly indicate that the YSK12-MEND represents a promising delivery system of siRNA for DC-based therapy, and will serve as valuable tool for future immunological and biological research directed at DCs

2. Materials and Methods

2.1. Materials.

YSK12-C4 was synthesized following the procedures presented in Supporting Information Scheme S1. 1,2-Dioleoyl-*sn*-glycero-3-phosphoethanolamine (DOPE) and cholesterol were purchased from Avanti Polar Lipids Inc. (Alabaster, AL). Phosphatidic acid (PA) and ovalbumin (OVA) (grade VI) were obtained from SIGMA-Aldrich Co. (St. Louis, MO). Cholesteryl GALA (Chol-GALA) and STR-R8 were synthesized by KURABO (Osaka, Japan). 1,2-dimyristoyl-*sn*-glycerol methoxyethyleneglycol 2000 ether (PEG-DMG) was purchased from NOF Corporation (Tokyo, Japan). RNAiMAX was also obtained from Life Technologies (Carlsbad, CA). Peptide SIINFEKL (major histocompatibility complex class I epitope of OVA) was synthesized by the Toray Research Center (Tokyo, Japan).

2.2. Cell line and animal.

E.G7-OVA cells, the murine lymphoma cell line EL4 expressing chicken OVA, were purchased from the American Type Culture Collection (Manassas, VA) and were cultured in RPMI 1640 medium containing 50 μ M 2-mercaptoethanol, 10 mM HEPES,

1 mM sodium pyruvate, 100 units/mL penicillin-streptomycin and 10% fetal bovine serum (FBS).

Female C57BL/6J mice (6-8 weeks old) were purchased from CLEA Japan Inc. (Tokyo, Japan) and maintained under specific pathogen-free conditions. The use of the mice was approved by the Pharmaceutical Science Animal Committee of Hokkaido University.

2.3. Preparation of YSK12-MEND and R8/GALA-MEND_{SUV}.

YSK12-MEND was prepared by the t-BuOH dilution procedure [23]. The YSK12-MEND was composed of YSK12-C4, cholesterol and PEG-DMG (85/15/1 molar ratio). PEG-DMG was used for stabilization of lipid membrane during the formulation process and for preservation of aggregation. Lipids were dissolved in a 90% t-BuOH solution at a concentration of 0.5 mM. DiI was added at 1 mol% of the total lipid, when DiI-labeled YSK12-MEND was prepared. The solution containing 600 nM siRNA was added to the lipid solution with vortexing and the mixture was quickly diluted with citrate buffer (pH 6.0) to a final concentration of <20% t-BuOH. The residual t-BuOH was replaced with PBS (pH 7.4), resulting in concentrating the YSK12-MEND. The pKa of the YSK12-MEND was 8.0, as measured by a TNS assay [23].

The R8/GALA-MEND_{SUV} was prepared as described previously [15,16]. Briefly, 0.55 mM SUVs composed of DOPE and PA (7:2 molar ratio) were mixed with siRNA/STR-R8 complex (2.46 nM siRNA) at a volume ratio of 2 : 1 (v/v). Finally, STR-R8 was added to the mixture at 10 mol% of total lipid. The diameter, polydispersity index (PDI), zeta-potential of R8/GALA-MEND_{SUV} were 115 ± 6 nm, 0.165 ± 0.015 and 36.5 ± 1.5 mV, respectively.

The diameter of the MENDs was determined by dynamic light scattering, and zeta potentials were determined by laser-Doppler velocimetry with a ZETASIZER Nano (ZEN3600, Malvern Instruments Ltd., Malvern, WR, UK). The diameter and zeta potential of the MENDs were measured when 10 mM HEPES buffer (pH 7.4) was used. The diameter, PDI and zeta-potential of the YSK12-MEND in 10 mM Tris-HCl buffer (pH 9.0) were 155 ± 4 nm, 0.064 ± 0.032 and 0.03 ± 0.74 mV, respectively.

2.4. RiboGreen assay.

The siRNA encapsulation efficiency of YSK12-MEND was determined by a RiboGreen assay [23]. The fluorescence of YSK12-MEND solution containing a 20 μ g/mL dextran sulfate and RiboGreen (Life Technologies) was measured by EnSpire

2300 Multilabel Reader (PerkinElmer, Waltham, MA) (Ex: 500 nm, Em: 525 nm). The encapsulation efficiency of siRNA was calculated by comparing the siRNA concentration in the presence and absence of 0.1 w/v% Triton X-100.

2.5. Transmission electron microscopy (TEM) observation

The YSK12-MEND was absorbed to formvar-coated copper grids (400 mesh) and then stained with a 2% phospho tungstic acid solution (pH 7.0) for 15 sec. The stained sample was observed by TEM (JEM-1400Plus; JEOL Ltd., Tokyo, Japan) at an acceleration voltage of 80 kV. Digital images (2048×2048 pixels) were obtained with a CCD camera (VELETA; Olympus Soft Imaging Solutions GmbH, Munster, Germany).

2.6 Culture of mouse bone-marrow derived DCs (BMDCs)

BMDCs were prepared as reported previously [24]. Briefly, bone marrow cells were collected from mice and the non-adherent cells were cultured in RPMI1640 medium containing 50 μM 2-mercaptoethanol, 10 mM HEPES, 1 mM sodium pyruvate, 100 U/mL penicillin-streptomycin, 10% FBS and 10 ng/mL granulocyte-macrophage colony-stimulating factor (GM-CSF) (R&D Systems, Basel, Switzerland) (culture medium). On days 2 and 4, non-adherent cells were washed out, and adherent cells were cultured in fresh culture medium. On day 6, non-adherent and loosely adherent cells were used as immature BMDCs. The analysis by flow cytometry showed that more than 85% of the cell population was CD11c positive.

2.7 Evaluation of gene silencing activity against scavenger receptor class B type 1 (SR-B1) gene in BMDCs

The evaluation of gene silencing of SR-B1 was performed as reported previously [16,25]. Anti-SR-B1 siRNA (5'-GUCGCAUGGCUCAGAGAGUTT-3', 5'-ACUCUCUGAGCCAUGCGACTT-3') was synthesized by Hokkaido System Science Co., Ltd. (Sapporo, Japan). BMDCs (6.0×10^5 cells) were seeded to 12 well plate and each carrier was added to the cells at siRNA doses of 0.3-100 nM. The cells were then incubated for 2 h at 37°C in 0.5 mL of serum-free OPTI-MEM I containing 10 ng/mL GM-CSF. After a 2 h incubation period, 0.5 mL of culture medium containing GM-CSF was added to the cells, followed by a further incubation for 24 h. After the incubation, BMDCs were collected and used for mRNA isolation by RNeasy Mini Kit (QIAGEN, Hilden, Germany) according the manufacturer's instructions. Briefly, the DNA contamination in the total RNA was eliminated by the DNase I treatment. The total RNA was then reverse-transcribed using a PrimeScript reverse

transcription (RT) reagent Kit (Takara Bio Inc., Shiga, Japan) with oligo-dT primer. Quantitative polymerase chain reaction (PCR) was performed with a Mx3000P QPCR System (Agilent Technologies, Santa Clara, CA) in 25 μ L aliquots of reaction mixures containing cDNA, appropriate pairs of primers and SYBR Green Realtime PCR Master Mix (TOYOBO Co., Osaka, Japan). SR-B1 level was calculated by the comparative C_T method using glyceraldehyde-3-phosphate dehydrogenase (GAPDH) as endogenous housekeeping genes. The following primer pairs were used: GAPDH: 5'-AACTTTGGCATTGTGGAAGG-3' (forward); 5'-GTCTTCTGGGTGGCAGTGAT-3' (reverse); SR-B1: 5'-TCCAGCCTGACAAGTCGCATGG-3' (forward); 5'-GCTTGCTCTCCATCAATATCGAGCC-3' (reverse).

2.8 Analysis of cytotoxicity

The analysis of cytotoxicity was performed by CellTiter 96 Aqueous One Solution Cell Proliferation Assay (Promega, Madison, WI). BMDCs (1.0×10^5 cells) were treated with each carrier at siRNA concentrations of 10, 30 and 100 nM in 0.1 mL of serum-free OPTI-MEM I in 96 well plate. CellTiter 96 Aqueous One Solution Reagent (20 μ L) was then added to each well. After the 2h incubation, the absorbance at 450 nm was measured and used to calculate cell viability (the absorbance of non-treatment was set to 100%).

2.9 Evaluation of cellular uptake.

BMDCs (2.0×10^5 cells) were incubated with each DiI-labeled carrier at siRNA concentrations of 10, 25, 50 and 100 nM for 30 min at 37°C in 0.1 mL of serum-free OPTI-MEM I in microtube. After the incubation, the part of the preparation was collected as the total fraction and the extra preparation was then centrifuged, after which a cell fraction and a supernatant fraction were obtained. The cell fraction was washed with 20 U/ml heparin in PBS. Reporter Lysis Buffer (Promega) was added to the total fraction, the cell fraction and the supernatant fraction. After a freeze-thaw cycle, the fluorescent intensity (FI) of each fraction was measured by EnSpire 2300 Multilabel Reader with $\lambda_{ex} = 549$ nm, $\lambda_{em} = 565$ nm. The uptake amount of siRNA (pmol) = siRNA dose (pmol) \times (FI of cell fraction / FI of total fraction).

2.10. Hemolysis assay.

Hemolysis assays were performed as reported previously [23]. Mouse red blood cells (RBCs) suspended with PBS were mixed with each quantity of siRNA

carriers at final siRNA concentrations of 0, 60, 120, 240 nM. After the mixtures were incubated at 37°C for 30 min, the absorbance at 545 nm of the supernatant was measured. The samples in the presence of 0.5 w/v% Triton X-100 were used as a positive control. The percentage of hemolysis activity was represented as the percentage of the absorbance of the positive control.

2.11. Evaluation of cathepsin B release to the cytosol.

Cathepsin B activity was measured with Cathepsin B Activity Assay Kit (Fluorometric) (abcam, Cambridge, UK). BMDCs (1.0×10^6 cells) were treated with each carrier at siRNA concentrations of 10, 30 and 100 nM for 2 h at 37°C in 0.5 mL of serum-free OPTI-MEM I in microtube. After the incubation, the cells were collected by centrifugation and suspended in 0.5 mL of ice-cold PBS. Digitonin solution was then added to the cell suspension. The permeabilization of only the plasma membrane was performed by treatment with a 32 µg/mL digitonin solution, whereas that of cell membrane and endosomal membrane was performed using a 200 µg/mL digitonin solution. After incubation for 15 min on ice, the supernatant was collected by centrifugation. 50 µL of the supernatant was mixed with 50 µL of cathepsin B substrate reagent in 96 well plate, followed by incubation for 2 h at 37°C. Finally, FI was measured by EnSpire 2300 Multilabel Reader with $\lambda_{ex} = 400$ nm, $\lambda_{em} = 505$ nm. The FI of no treatment cells treated with 32 µg/mL digitonin was set to 0% of cathepsin B activity, whereas the FI of the cells treated with 200 µg/mL digitonin was set to 100% of cathepsin B activity.

2.12. Evaluation of gene silencing activity against SOCS1 gene in BMDCs

The evaluation of SOCS1 gene silencing was performed as reported previously [15]. Anti-SOCS1 siRNA (5'-GAGAACCUGGCGCGCAUCCUCUUA-3', 5'-UAAGAGGGAUGCGCGCCAGGUUCUC-3') was obtained from Life Technologies. Anti-human PLK1 siRNA as a control siRNA (5'-AGAuCACCCuCCUAAAuAUU-3', 5'-UAUUUAAGGAGGGUGAuCUUU-3', 2'-OMe-modified nucleotides are in lowercase.) was synthesized by Hokkaido System Science Co., Ltd. BMDCs (6.0×10^5 cells) were incubated with each carrier at siRNA concentrations of 3, 10 and 30 nM for 2 h at 37°C in 0.5 mL of serum-free OPTI-MEM I containing 10 ng/mL GM-CSF in 12 well plate. After the 2 h incubation, 0.5 mL of culture medium was added to the cells, followed by a further incubation for 2 h. IFN- γ was then added to the cells at a concentration of 50 ng/mL, followed by further incubation for 24 h. After the incubation, the cells and the supernatant were collected

and used for the evaluation of gene knockdown and the quantification of cytokine production, respectively. The evaluation of gene knockdown was conducted as well as previously described method. SOCS1 level was calculated by the comparative C_T method using GAPDH as endogenous housekeeping genes. The SOCS1 primer pairs were used: 5'-ACCTTCTTGGTGCGCGAC-3' (forward); 5'-AAGCCATCTTCACGCTGAGC-3' (reverse). The concentration of tumor necrosis factor α (TNF- α) and interleukin 6 (IL-6) in the supernatant was measured by Quantikine ELISA kit (R&D Systems). The measurement was carried out following the manufacturer's instructions.

2.13. Evaluation of antitumor effect mediated by SOCS1-silenced BMDCs.

The SOCS1-silenced BMDCs were prepared as follows. BMDCs (6.0×10^5 cells) were incubated with each anti-SOCS1 siRNA-loaded carrier at siRNA concentration of 30 nM for 2 h at 37°C in 0.5 mL of serum-free OPTI-MEM I containing 10 ng/mL GM-CSF in 12 well plate. After the 2 h incubation, 0.5 mL of culture medium was added to the cells, followed by a further incubation for 2 h. After the incubation, the cells were washed with culture medium and suspended in fresh culture medium, followed by a further incubation for 2 h. The cells were then pulsed with the SIINFEKL peptide (750 nM) and OVA (50 μ g/mL) at 37°C for 30 min, followed by stimulation with polyI:C (SIGMA-Aldrich Co) (500 ng/mL) for 1 h to develop mature BMDCs. For a preventative experiment, the mice were immunized by an injection of 4.0×10^5 mature BMDCs into the hind footpads. At 7 days after the immunization, 1.0×10^6 E.G7-OVA cells were subcutaneously inoculated into the right flank of the mice. For a therapeutic experiment, the mice were subcutaneously inoculated with 1.0×10^6 E.G7-OVA cells. On days 4, 7, and 15, the mice were immunized by an injection of 3.0×10^5 mature BMDCs into the hind footpads. Tumor volume = (major axis \times minor axis²) \times 0.52.

2.14. Statistical Analysis.

Statistical analysis of multiple comparisons were performed by one-way or two-way ANOVA, followed by the Tukey-Kramer test or Dunnett test (Fig. 4b, c). A P value of <0.05 was considered to be a significant difference.

3. Results and Discussion

3.1. Synthesis of YSK12-C4 and preparation of YSK12-MEND

To enhance in vitro siRNA transduction, YSK12-C4 was designed so as to have a cationic property and unsaturated carbon chains, based on YSK05 (Fig. 1a). The yield of YSK12-C4 was 64% (Scheme S1, Supporting information). YSK05 (Fig. S1), a pH-sensitive cationic lipid, enhances the ability of the MEND to escape from endosomes and showed efficient gene silencing in liver in vivo [23]. YSK05 contains one tertiary amine conferring pH-sensitive properties of MEND (pKa 6.6), and two double bonds per acyl chain for emphasizing fusion with the endosomal membrane. Although the pKa of YSK05-MEND is useful for conferring stability in the blood circulation, it can be a disadvantage for in vitro siRNA delivery. Moreover, the pH of endocytic vesicles in DCs appears to be retained in a neutral or mildly acidic environment and the acidification appears to be slow, when DCs internalize antigens [21,22]. Therefore, we designed the YSK12-C4, with different properties from YSK05. To overcome the above problems, it was necessary to create a MEND that is positively charged under extracellular conditions and in endocytic vesicles of DCs. This was accomplished by increasing pKa of an alkyl chain that was introduced in the particle, in place of the cyclic ketal. The replacement also would decrease the sterical demand imposed on the head group of the lipid, resulting in an enhancement in the fusogenic capability of the MEND.

The YSK12-MEND was prepared by the t-BuOH dilution method. The t-BuOH dilution method prepares small and uniform particles and efficiently encapsulates siRNA [23]. The YSK12-MEND is composed of YSK12-C4, cholesterol and PEG-DMG (85:15:1, molar ratio) (Fig. 1b). The values for the diameter, PDI and zeta-potential of the YSK12-MEND at physiological pH (pH 7.4) were 180 ± 6 nm, 0.072 ± 0.024 and 5.8 ± 0.6 mV, respectively. The YSK12-MEND had a weak positive charge. The siRNA encapsulation ratio of the YSK12-MEND was $94.2 \pm 0.8\%$. In a TEM observation, sub-200 nm sized nanoparticles were observed and the population appeared to be highly uniform (Fig. 1c). The particles appeared to be a structure in which the inside was filled with lipid. This result is consistent with a previous report using siRNA-loaded lipid nanoparticles [26].

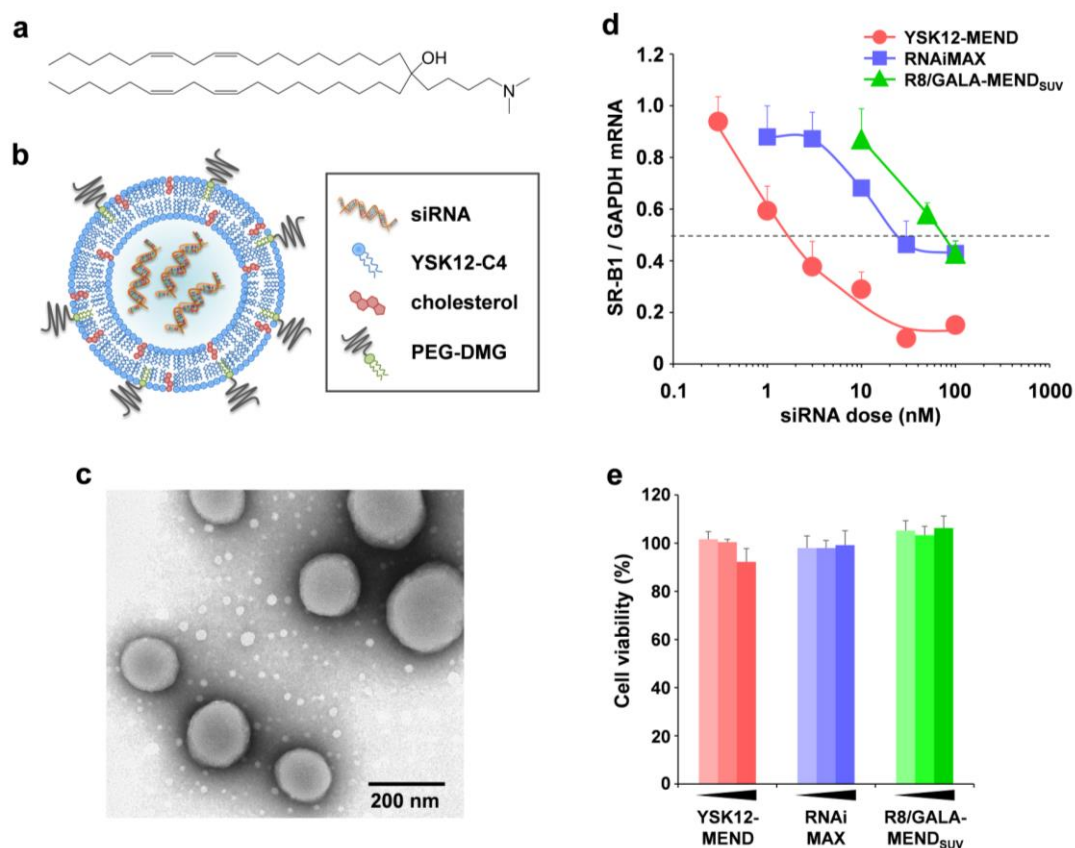


Fig. 1. Construction and functional analysis of the YSK12-MEND. (a) Chemical structural formula of YSK12-C4. (b) Conceptual image of YSK12-MEND. YSK12-MEND was composed of YSK12-C4, cholesterol and PEG-DMG (85/15/1 molar ratio). (c) TEM image of the YSK12-MEND. (d) Dose response curve for gene silencing efficiency against the SR-B1 gene in BMDCs. BMDCs were treated with the YSK12-MEND, RNAiMAX or R8/GALA-MEND_{SUV} and the mRNA levels of SR-B1 were measured by quantitative RT-PCR at 24 h after the treatment. The vertical axis shows the relative SR-B1/GAPDH mRNA level, in which the mean value of the no treatment BMDCs was assumed to be 1.0. Data are the mean \pm SEM (n=3-5). (e) Cell viability of BMDCs. BMDCs were treated with YSK12-MEND, RNAiMAX or R8/GALA-MEND_{SUV} (siRNA doses of 3, 10, 100 nM) and the cell viability was measured at 2 h after the treatment. Data are the mean \pm SEM (n=3).

3.2. Evaluation of YSK12-MEND for siRNA transduction into BMDCs

The gene silencing activity of the YSK12-MEND in BMDCs was compared with RNAiMAX and R8/GALA-MEND_{SUV}. RNAiMAX is one of the most powerful reagents for in vitro siRNA transduction, and is commercially available. The SR-B1 gene was used as a siRNA target gene, since it is expressed in BMDCs as an endogenous gene. The YSK12-MEND showed dose dependent gene silencing activity and the ED₅₀ for the gene silencing activity was 1.5 nM siRNA (Fig. 1d). In addition, the YSK12-MEND yielded a high transfection efficiency with a >90% knockdown at 30 nM siRNA. On the other hand, the ED₅₀ of RNAiMAX and R8/GALA-MEND_{SUV} were

25 nM siRNA and 70 nM siRNA, respectively (Fig. 1d). The ED₅₀ of YSK12-MEND was one order magnitude lower than the values for RNAiMAX and R8/GALA-MEND_{SUV}. Even at an siRNA concentration of 100 nM, the transfection efficiencies of RNAiMAX and R8/GALA-MEND_{SUV} were 57% and 57%, respectively. In lipid nanoparticles containing an ionizable cationic lipid, DLin-KC2-DMA, (KC2-LNP), a siRNA dose of more than 125 nM was needed for efficient gene silencing, although KC2-LNP is one of the most powerful siRNA delivery systems [14,27]. The KC2-LNP and YSK05-MEND showed efficient gene silencing in the liver in vivo. These facts indicate that the strategy for the KC2-LNP and YSK05-MEND, namely the enhancement of endosomal escape by a pH-sensitive lipid, can be insufficient for efficient gene silencing in DCs. This finding suggests that the YSK12-MEND is superior to commercial reagents or reported delivery systems that are currently used for gene silencing in DCs. In addition to the evaluation of knockdown efficiency, we also investigated the cytotoxicity of YSK12-MEND against BMDCs. After siRNA transduction, cell viability was evaluated in the same siRNA dose range by a MTS chromogenic assay, a method to measure the activity of living mitochondria. The lipid/siRNA mol ratio of the YSK12-MEND and the R8/GALA-MEND_{SUV} were 842 lipid/siRNA and 476 lipid/siRNA, respectively. In a cytotoxic assay, the lipid concentrations of the YSK12-MEND and the R8/GALA-MEND_{SUV} were as follows: YSK12-MEND (2.5, 8.4 and 84.2 μM); R8/GALA-MEND_{SUV} (1.4, 4.8 and 47.6 μM). As a result, the YSK12-MEND showed no cytotoxicity as well as RNAiMAX and R8/GALA-MEND_{SUV} in the range of < 100 nM (Fig. 1e). This result confirms the absence of cytotoxicity of the YSK12-MEND at the dose range required to achieve sufficient gene silencing. The low level of toxicity of YSK12-MEND is quite favorable for DC-based therapy, and also biological research.

3.3. Quantitative analysis of cellular uptake of YSK12-MEND in BMDCs

We next evaluated siRNA trafficking in BMDCs by the YSK12-MEND, RNAiMAX and R8/GALA-MEND_{SUV}. In general, the siRNA-mediated silencing was improved, probably due to either an increased siRNA uptake into cells or the effectiveness of endosomal escape into the cytoplasm. To evaluate the cellular uptake of the carriers, we used DiI, a fluorescent compound that intercalates into lipid membranes, and, based on this, we calculated amount of siRNA taken up using the formula described in the methods part. Before comparing the cellular uptake among the carriers, the amount of siRNA delivered by the YSK12-MEND was examined at 0.5, 1, 2, 4 and 6 h after the treatment. As a result, the amount of siRNA taken up was essentially the

same at all time points (Fig. S2, Supporting Information). In addition, there was a concern that fluorescent attenuation with time could result in an inaccurate evaluation. Thus, the cellular uptake of carriers was evaluated at 30 min post-transfection. As a result, there was no significant difference in cellular uptake among the carriers at siRNA doses of 10, 25 and 50 nM, although the amount of siRNA taken up in the YSK12-MEND-treated BMDC was significantly lower than the values for the R8/GALA-MEND_{SUV} at a siRNA dose of 100 nM (Fig. 2). The difference in uptake efficiency appears to be due to the difference in the zeta-potential of carrier. The zeta-potential of the YSK12-MEND was 5.8 mV, whereas the zeta-potentials for R8/GALA-MEND_{SUV} were high (36.5 mV). RNAiMAX may also be high. The weak positive charge of the YSK12-MEND appeared to have only a minor effect on the cellular uptake process in BMDCs. Consequently, this fact indicates that the amount of siRNA taken up by BMDCs may not be responsible for high silencing activity of the YSK12-MEND.

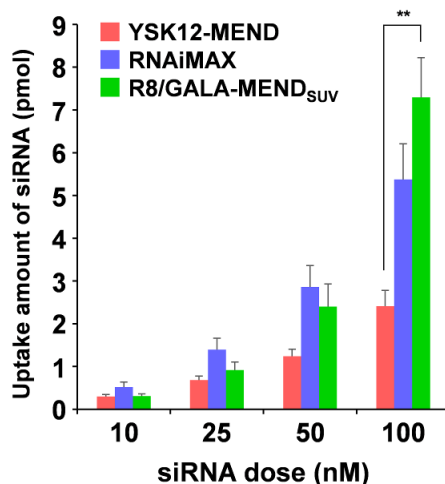


Fig. 2. Quantitative analysis of cellular uptake of the YSK12-MEND. BMDCs were treated with DiI-labeled the YSK12-MEND, RNAiMAX or R8/GALA-MEND_{SUV}. The fluorescence intensity in the cells was measured at 30 min after the treatment. Data are the mean \pm SEM (**P<0.01, n=3).

3.4. High potency of endosome disruption by YSK12-MEND

We next focused on the endosomal escape step in the process. The fusogenicity of nanoparticles is important for enhancing endosomal escape [17]. We previously showed that a MEND containing YSK05 results in an enhanced endosomal escape via membrane disruption [23]. The potency of the YSK12-MEND to induce membrane

disruption was first evaluated by means of a hemolysis assay at pH5.5, 6.5 and 7.4. In the hemolysis assay, we investigated the function of YSK12-MEND, including membrane disruption activity, against lipid membranes *in vitro* (in a test tube). To examine the siRNA dose needed to show a maximum effect by the YSK12-MEND, a high dose range of siRNA (0-240 nM) was used. As shown in Fig. 3a, the YSK12-MEND and the R8/GALA-MEND_{SUV} both induced membrane disruption depending on the dose of siRNA, while membrane disruption was independent of pH. The potency of membrane disruption of YSK12-MEND appears to be higher than that of the R8/GALA-MEND_{SUV}. YSK12-MEND showed a maximum effect (100% hemolytic activity) at a siRNA dose of 240 nM. On the other hand, RNAiMAX showed only minor hemolytic activity. This suggests that the YSK12-MEND induced efficient membrane disruption against lipid membranes. Meanwhile, the strong hemolytic activity of the YSK12-MEND appears to influence cytotoxicity. As shown in Fig. 1e, it is likely that some cells were damaged by the YSK12-MEND at a siRNA dose of 100 nM, although the decrease in cell viability was not significant. Although it is difficult to discuss the influence based on the dose of siRNA used because the experimental conditions and sensitivity of the hemolytic assay are different from those for the cytotoxic assay, the cytotoxicity appears to be due to the strong membrane disruption activity of the YSK12-MEND. However, this possible cytotoxicity does not appear to be serious, because the YSK12-MEND induced sufficient gene silencing at a siRNA dose of 30 nM.

Subsequently, to investigate the membrane disruption activity of the YSK12-MEND against endosomal membranes of BMDCs at siRNA dose range (10-100 nM) at which sufficient gene silencing is induced, the disruption of endosomes in BMDCs was examined by detecting the leakage of cathepsin B from endosomes. Cathepsin B is a cysteine endoprotease and is normally localized in endosomes [28]. When endosomes are disrupted, cathepsin B will leak into the cytosol. Thus, the presence of cathepsin B in the cytosol is an indicator of the extent of disruption of endosomes [29,30]. To examine the amount of cathepsin B released from endosomes to the cytosol, the plasma membrane was made permeable by a digitonin treatment. The plasma membrane to be partially damaged and increases its permeability [31,32]. We optimized the concentration of digitonin to induce membrane penetration in only the plasma membrane, but not endosomal membranes (Fig. 3b). At 2 h post-treatment with each siRNA carrier, the cells were treated with digitonin and the cathepsin B activity in the supernatant was measured (Fig. 3b). As a result, a high cathepsin B activity was observed in the cells that had been treated with the YSK12-MEND compared with the

cells treated with RNAiMAX or R8/GALA-MEND_{SUV} (Fig. 3c). The cathepsin B activity induced by YSK12-MEND was dependent on the dose of siRNA. This finding indicates that the YSK12-MEND drastically enhances the disruption of the endosomal membrane compared with RNAiMAX or R8/GALA-MEND_{SUV}. In particular, the cathepsin B activity of YSK12-MEND at a siRNA dose of 30 nM, the typical dose used in the subsequent experiments, was 11 times higher than those for RNAiMAX and R8/GALA-MEND_{SUV}. This suggests that the efficient gene silencing by the YSK12-MEND can be attributed to an enhancement in endosomal escape via membrane disruption. On the other hand, a very low level of cathepsin B activity was observed in cells treated with RNAiMAX or the R8/GALA-MEND_{SUV}. This suggests that the RNAiMAX and R8/GALA-MEND_{SUV} are not sufficiently potent to induce the leakage of cathepsin B from endosomes. However, the R8/GALA-MEND_{SUV} induced a high hemolytic activity (Fig. 3a). This contradiction might be due to the difference in the cells used in the experiment. The results shown in Fig. 3c appear to reflect the environment of siRNA transfection, compared with that of Fig. 3a.

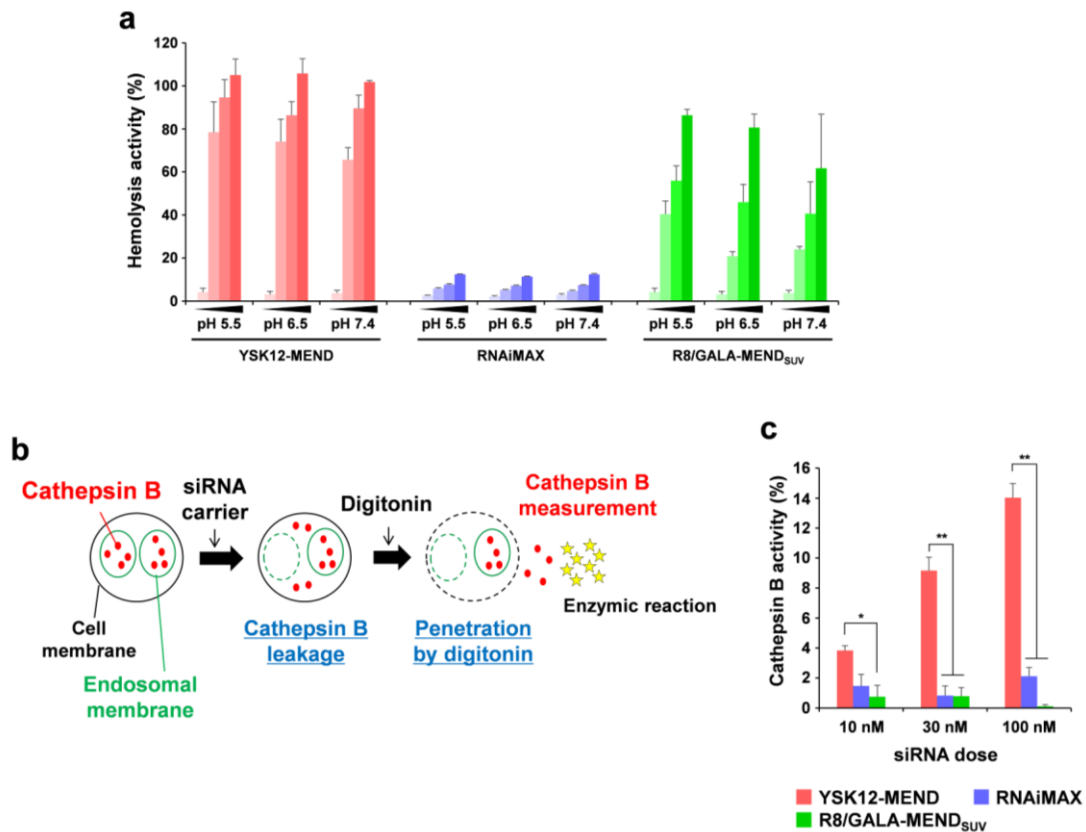


Fig. 3. Analysis of membrane disruption activity of the YSK12-MEND. (a) Hemolysis assay.

RBC suspension was mixed with YSK12-MEND, RNAiMAX or R8/GALA-MEND_{SUV} at final siRNA concentrations of 0, 60, 120, 240 nM and the mixtures were incubated for 30 min at 37°C. The absorbance due to hemoglobin was measured. Data are the mean \pm SEM (n=3). (b) Scheme of analysis of cathepsin B release to the cytosol. (c) Analysis of cathepsin B activity in the cytosol. BMDCs were treated with YSK12-MEND, RNAiMAX or R8/GALA-MEND_{SUV} at siRNA doses of 10, 30 and 100 nM and the activity of cathepsin B released to the cytosol was measured at 2 h after the treatment. Data are the mean \pm SEM (**P<0.01, n=3).

3.5. Enhancement of immune response in SOCS1-silenced BMDCs by YSK12-MEND

We next investigated the potential of the YSK12-MEND for the control of DC functions and DC-based therapy mediated by RNAi. SOCS1 negatively regulates the cytokine responses in immune cells and the expression is induced by cytokine stimuli. Blocking Janus kinase (JAK)-signal transducers, and activators of transcription (STAT) signaling pathways is responsible for the negative-feedback of immune responses by SOCS, leading to the immunosuppression of DCs [33]. Thus, the knockdown of the SOCS1 gene by siRNA enhances the immune functions of DCs [3]. We first evaluated the gene silencing efficiency of SOCS1 by the YSK12-MEND in BMDCs. The YSK12-MEND showed significant knockdown of the SOCS1 gene compared with RNAiMAX and R8/GALA-MEND_{SUV} at siRNA doses of 3, 10 and 30 nM (Fig. 4a). Of note, the silencing efficiency of YSK12-MEND was more than 80% at a siRNA dose of 3 nM. This silencing efficiency appear to be similar to that of the lentivirus vector [3]. On the other hand, in this range of siRNA doses, both the RNAiMAX and R8/GALA-MEND_{SUV} failed to induce a 50% higher gene silencing efficiency. This result clearly indicates that the YSK12-MEND induces a drastic silencing efficiency of immunosuppressive genes in BMDCs, compared with other non-viral vectors.

To further evaluate the enhancement in DC functions by the knockdown of the SOCS1 gene, the productions of TNF- α and IL-6 induced by IFN- γ stimulation were examined in SOCS1-silenced BMDCs. No enhancement of TNF- α and IL-6 production was observed in cells treated with RNAiMAX and R8/GALA-MEND_{SUV} compared with vehicle (Fig. 4b, c). On the other hand, the SOCS1-silenced BMDCs by the YSK12-MEND significantly enhanced TNF- α (30 nM siRNA) and IL-6 (10 and 30 nM siRNA) production (Fig. 4b, c). These findings suggest that the siRNA delivery mediated by YSK12-MEND efficiently cancels the immunosuppression and enhances the immune responses in BMDCs.

Although the silencing efficiencies of the YSK12-MEND as a function of the siRNA dose were not significant different, a significant enhancement of cytokine production was observed only at siRNA doses of 10 nM (IL-6) and 30 nM (TNF- α and IL-6). The possible reason for this inconsistency appears to be due to differences in the

dose response curve between gene silencing efficiency and cytokine concentration. Given that SOCS1 shows a very efficient suppressive effect for IFN- γ signaling even at low levels of SOCS1 expression [34], the dose response curve for cytokine concentration is possibly present at the right side of the dose response curve for gene silencing efficiency. Thus, a difference in cytokine production was observed between 3 nM siRNA and 30 nM siRNA.

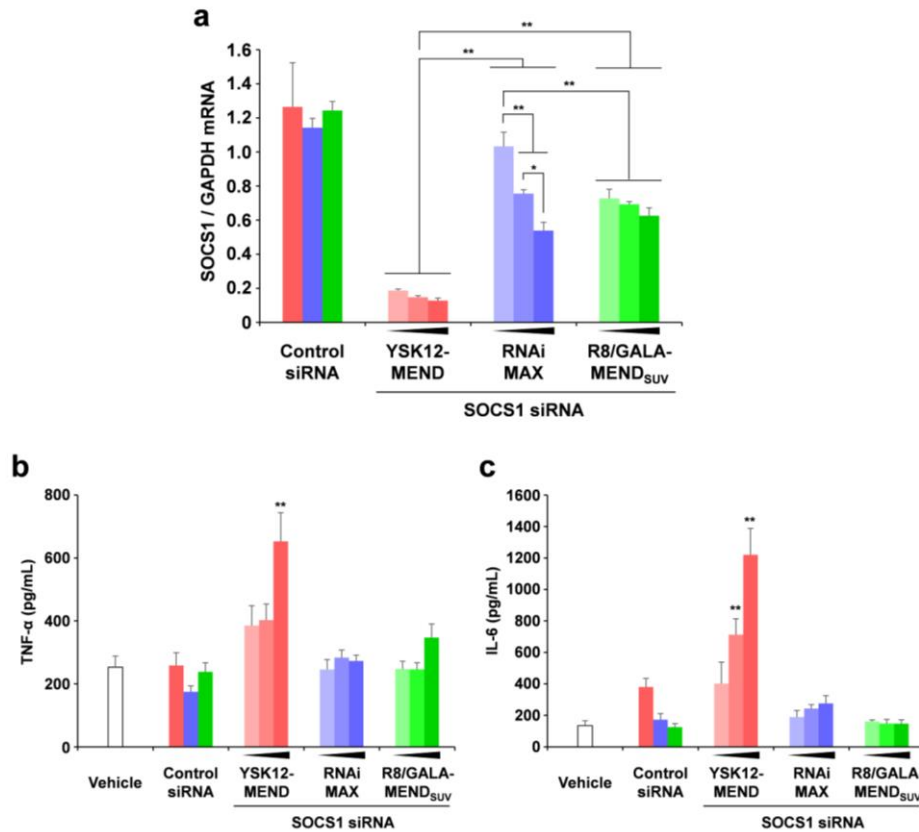


Fig. 4. Analysis of immune responses in SOCS1-silenced BMDCs by the YSK12-MEND. BMDCs were treated with YSK12-MEND, RNAiMAX or R8/GALA-MEND_{SUV}. The anti-SOCS1 siRNA doses were 3, 10 and 30 nM. The control siRNA (anti-human PLK1 siRNA) dose was 30 nM. (a) Gene silencing against SOCS1 in BMDCs. The mRNA levels of SOCS1 were measured by quantitative RT-PCR at 30 h after the treatment. The vertical axis shows the relative SOCS1/GAPDH mRNA level, in which the mean value of the no treatment BMDCs was assumed to be 1.0. Data are the mean \pm SEM (**P<0.01, *P<0.05, n=3). The concentration of TNF- α (b) and IL-6 (c) in the supernatant at 30 h after the treatment was measured by ELISA. Data are the mean \pm SEM (**P<0.01 v.s. vehicle, n=3).

3.6. Cancer immunotherapy using SOCS1-silenced BMDCs by YSK12-MEND

The SOCS1-silenced BMDCs by YSK12-MEND is expected to facilitate the effect of DC-based therapy. Thus, we finally examined the potential of the SOCS1-silenced BMDCs by the YSK12-MEND for use in cancer immunotherapy. To

examine a preventative antitumor effect, mice were immunized with SOCS1-silenced BMDCs, control siRNA treated BMDCs and PBS and then inoculated with E.G7-OVA cells. As a result, the mice groups immunized with SOCS1-silenced BMDC by the RNAiMAX or R8/GALA-MEND_{SUV} showed a significant inhibition of tumor growth compared with each of the control groups, whereas the establishment of tumors was observed in the both groups (Fig. 5a). Of note, the treatment of SOCS1-silenced BMDC by the YSK12-MEND completely inhibited tumor engraftment, although the establishment of tumors was observed in the mice group that had been immunized with the BMDC treated with control siRNA-loaded YSK12-MEND (Fig. 5a). This result indicates that the immunization of SOCS1-silenced BMDC by the YSK12-MEND efficiently induces antigen-specific antitumor immunity only by one immunization. In a previous report, the immunization of SOCS1-silenced BMDC by R8/GALA-MEND_{SUV} failed to completely inhibit tumor growth, even when the BMDC was transfected with R8/GALA-MEND_{SUV} at a siRNA dose of 80 nM [15]. Thus, these facts clearly indicate that the capability of the YSK12-MEND is markedly superior in comparison with R8/GALA-MEND_{SUV}.

Subsequently, we investigated the therapeutic antitumor effect of SOCS1-silenced BMDC by the YSK12-MEND. It should be noted that a therapeutic antitumor effect was not observed in our previous trial, when the SOCS1-silenced BMDC involved the use of the R8/GALA-MEND_{SUV} at a siRNA dose of 80 nM was injected to mice (unpublished data). Thus, in the case of therapeutic experiment, the YSK12-MEND was compared with RNAiMAX. Mice were inoculated with E.G7-OVA cells. On days 4, 7 and 15, the mice were immunized with SOCS1-silenced BMDCs, control siRNA treated BMDCs and PBS. As a result, the mice group that had been immunized with SOCS1-silenced BMDC by YSK12-MEND showed a significant inhibition of tumor growth compared with the control groups, whereas the mice group immunized with SOCS1-silenced BMDC by RNAiMAX did not (Fig. 5b). This result also reflects the high capability of the YSK12-MEND compared with other non-viral vectors.

These antitumor effects can be attributed to the enhancement of immune functions of BMDC caused by high SOCS1 silencing by the YSK12-MEND. Therefore, these results clearly show that YSK12-MEND is a promising siRNA carrier that can enhance DC-based therapy.

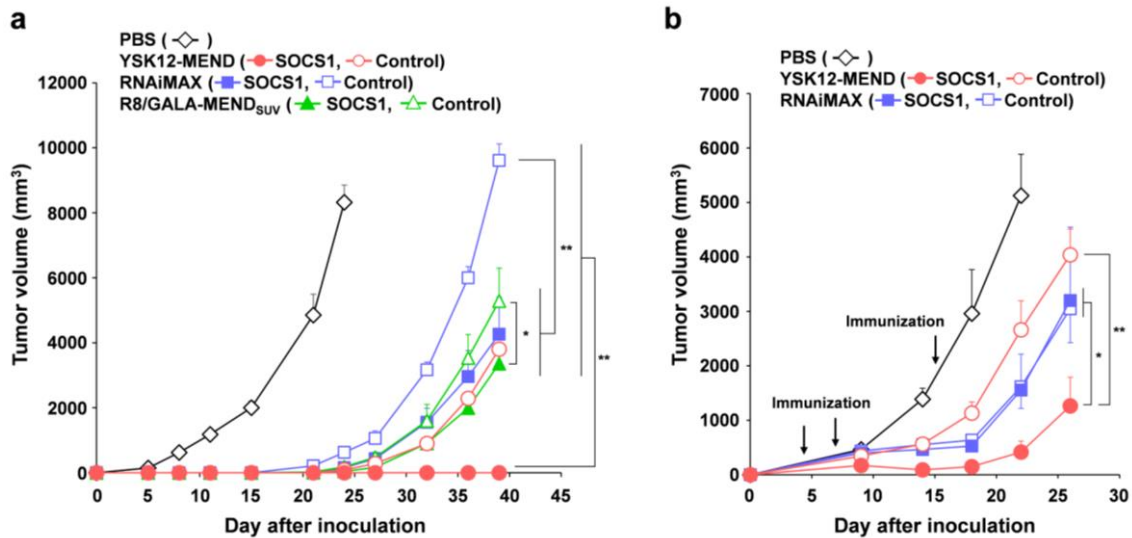


Fig. 5. Antitumor effect mediated by SOCS1-silenced BMDCs by the YSK12-MEND. (a) Preventative antitumor effect. Mice were immunized with BMDCs treated with the YSK12-MEND, RNAiMAX or R8/GALA-MEND_{SUV}. The dose of anti-SOCS1 siRNA and control siRNA (anti-human PLK1 siRNA) was 30 nM. At 7 days after the immunization, E.G7-OVA cells were inoculated to the immunized mice and tumor growth was monitored. Data are the mean \pm SEM (** $P < 0.01$, * $P < 0.05$, $n = 3-5$). (b) Therapeutic antitumor effect. Mice were inoculated with E.G7-OVA cells. On days 4, 7 and 15, the mice were immunized with BMDCs treated with the YSK12-MEND or RNAiMAX and the tumor growth was monitored. The dose of anti-SOCS1 siRNA and control siRNA (anti-human PLK1 siRNA) was 30 nM. Data are the mean \pm SEM (** $P < 0.01$, * $P < 0.05$, $n = 5$).

4. Conclusions

The results of the present study show that a MEND containing the new cationic lipid YSK12-C4, YSK12-MEND, is a highly potent non-viral vector for the delivery of siRNA to DCs and enhances the effect of DC-based cancer immunotherapy by controlling the expression of immunosuppressive genes. The capability of YSK12-MEND was drastically superior to commercial reagents and reported non-viral vectors. Therefore, YSK12-MEND would be a breakthrough technology for siRNA delivery to DCs and be a useful non-viral vector for DC-based therapy and biological research.

Acknowledgements

This work was supported in part by JSPS KAKENHI Grant Numbers 26713002. We also appreciate Dr. Milton S. Feather for this helpful advice in writing the English manuscript.

References

- [1] S. Anguille, E. L. Smits, E. Lion, V. F. van Tendeloo, Z. N. Berneman. Clinical use of dendritic cells for cancer therapy. *Lancet Oncol* 15 (2014) e257-267.
- [2] M. L. Huber, L. Haynes, C. Parker, P. Iversen. Interdisciplinary critique of sipuleucel-T as immunotherapy in castration-resistant prostate cancer. *J Natl Cancer Inst* 104 (2012) 273-279.
- [3] L. Shen, K. Evel-Kabler, R. Strube, S. Y. Chen. Silencing of SOCS1 enhances antigen presentation by dendritic cells and antigen-specific anti-tumor immunity. *Nat Biotechnol* 22 (2004) 1546-1553.
- [4] X. T. Song, K. Evel-Kabler, L. Shen, L. Rollins, X. F. Huang, S. Y. Chen. A20 is an antigen presentation attenuator, and its inhibition overcomes regulatory T cell-mediated suppression. *Nat Med* 14 (2008) 258-265.
- [5] L. Yang, Y. Pang, H. L. Moses. TGF-beta and immune cells: an important regulatory axis in the tumor microenvironment and progression. *Trends Immunol* 31 (2010) 220-227.
- [6] C. Sheridan. IDO inhibitors move center stage in immuno-oncology. *Nat Biotechnol* 33 (2015) 321-322.
- [7] J. Jantsch, N. Turza, M. Volke, K. U. Eckardt, M. Hensel, A. Steinkasserer, C. Willam, A. T. Prechtel. Small interfering RNA (siRNA) delivery into murine bone marrow-derived dendritic cells by electroporation. *J Immunol Methods* 337 (2008) 71-77.
- [8] E. Marshall. Gene therapy death prompts review of adenovirus vector. *Science* 286 (1999) 2244-2245.
- [9] X. Gu, J. Xiang, Y. Yao, Z. Chen. Effects of RNA interference on CD80 and

- CD86 expression in bone marrow-derived murine dendritic cells. *Scand J Immunol* 64 (2006) 588-594.
- [10] M. H. Karimi, P. Ebadi, A. A. Pourfathollah, Z. S. Soheili, S. Samiee, Z. Ataei, S. Z. Tabei, S. M. Moazzeni. Immune modulation through RNA interference-mediated silencing of CD40 in dendritic cells. *Cell Immunol* 259 (2009) 74-81.
- [11] M. B. Heo, Y. T. Lim. Programmed nanoparticles for combined immunomodulation, antigen presentation and tracking of immunotherapeutic cells. *Biomaterials* 35 (2014) 590-600.
- [12] W. Jiang. Blockade of B7-H1 enhances dendritic cell-mediated T cell response and antiviral immunity in HBV transgenic mice. *Vaccine* 30 (2012) 758-766.
- [13] Q. Zhang, D. M. Hossain, S. Nechaev, A. Kozłowska, W. Zhang, Y. Liu, C. M. Kowolik, P. Swiderski, J. J. Rossi, S. Forman, S. Pal, R. Bhatia, A. Raubitschek, H. Yu, M. Kortylewski. TLR9-mediated siRNA delivery for targeting of normal and malignant human hematopoietic cells in vivo. *Blood* 121 (2013) 1304-1315.
- [14] W. Hobo, T. I. Novobrantseva, H. Fredrix, J. Wong, S. Milstein, H. Epstein-Barash, J. Liu, N. Schaap, R. van der Voort, H. Dolstra. Improving dendritic cell vaccine immunogenicity by silencing PD-1 ligands using siRNA-lipid nanoparticles combined with antigen mRNA electroporation. *Cancer Immunol Immunother* 62 (2013) 285-297.
- [15] H. Akita, K. Kogure, R. Moriguchi, Y. Nakamura, T. Higashi, T. Nakamura, S. Serada, M. Fujimoto, T. Naka, S. Futaki, H. Harashima. Nanoparticles for ex vivo siRNA delivery to dendritic cells for cancer vaccines: programmed endosomal escape and dissociation. *J Control Release* 143 (2010) 311-317.

- [16] S. Warashina, T. Nakamura, H. Harashima. A20 silencing by lipid envelope-type nanoparticles enhances the efficiency of lipopolysaccharide-activated dendritic cells. *Biol Pharm Bull* 34 (2011) 1348-1351.
- [17] K. Kajimoto, Y. Sato, T. Nakamura, Y. Yamada, H. Harashima. Multifunctional envelope-type nano device for controlled intracellular trafficking and selective targeting in vivo. *J Control Release* 190 (2014) 593-606.
- [18] T. Nakamura, H. Akita, Y. Yamada, H. Hatakeyama, H. Harashima. A multifunctional envelope-type nanodevice for use in nanomedicine: concept and applications. *Acc Chem Res* 45 (2012) 1113-1121.
- [19] K. Kogure, R. Moriguchi, K. Sasaki, M. Ueno, S. Futaki, H. Harashima. Development of a non-viral multifunctional envelope-type nano device by a novel lipid film hydration method. *J Control Release* 98 (2004) 317-323.
- [20] T. Kakudo, S. Chaki, S. Futaki, I. Nakase, K. Akaji, T. Kawakami, K. Maruyama, H. Kamiya, H. Harashima. Transferrin-modified liposomes equipped with a pH-sensitive fusogenic peptide: an artificial viral-like delivery system. *Biochemistry* 43 (2004) 5618-5628.
- [21] M. B. Lutz, P. Rovere, M. J. Kleijmeer, M. Rescigno, C. U. Assmann, V. M. Oorschot, H. J. Geuze, J. Trucy, D. Demandolx, J. Davoust, P. Ricciardi-Castagnoli. Intracellular routes and selective retention of antigens in mildly acidic cathepsin D/lysosome-associated membrane protein-1/MHC class II-positive vesicles in immature dendritic cells. *J Immunol* 159 (1997) 3707-3716.
- [22] K. Honda, Y. Ohba, H. Yanai, H. Negishi, T. Mizutani, A. Takaoka, C. Taya, T. Taniguchi. Spatiotemporal regulation of MyD88-IRF-7 signalling for robust

- type-I interferon induction. *Nature* 434 (2005) 1035-1040.
- [23] Y. Sato, H. Hatakeyama, Y. Sakurai, M. Hyodo, H. Akita, H. Harashima. A pH-sensitive cationic lipid facilitates the delivery of liposomal siRNA and gene silencing activity in vitro and in vivo. *J Control Release* 163 (2012) 267-276.
- [24] T. Nakamura, R. Moriguchi, K. Kogure, N. Shastri, H. Harashima. Efficient MHC class I presentation by controlled intracellular trafficking of antigens in octaarginine-modified liposomes. *Mol Ther* 16 (2008) 1507-1514.
- [25] T. Nakamura, Y. Fujiwara, S. Warashina, H. Harashima. The intracellular pharmacodynamics of siRNA is responsible for the low gene silencing activity of siRNA-loaded nanoparticles in dendritic cells. *Int J Pharm* 494 (2015) 271-277.
- [26] S. Ramishetti, R. Kedmi, M. Goldsmith, F. Leonard, A. G. Sprague, B. Godin, M. Gozin, P. R. Cullis, D. M. Dykxhoorn, D. Peer. Systemic Gene Silencing in Primary T Lymphocytes Using Targeted Lipid Nanoparticles. *ACS Nano* 9 (2015) 6706-6716.
- [27] S. C. Semple, A. Akinc, J. Chen, A. P. Sandhu, B. L. Mui, C. K. Cho, D. W. Sah, D. Stebbing, E. J. Crosley, E. Yaworski, I. M. Hafez, J. R. Dorkin, J. Qin, K. Lam, K. G. Rajeev, K. F. Wong, L. B. Jeffs, L. Nechev, M. L. Eisenhardt, M. Jayaraman, M. Kazem, M. A. Maier, M. Srinivasulu, M. J. Weinstein, Q. Chen, R. Alvarez, S. A. Barros, S. De, S. K. Klimuk, T. Borland, V. Kosovrasti, W. L. Cantley, Y. K. Tam, M. Manoharan, M. A. Ciufolini, M. A. Tracy, A. de Fogerolles, I. MacLachlan, P. R. Cullis, T. D. Madden, M. J. Hope. Rational design of cationic lipids for siRNA delivery. *Nat Biotechnol* 28 (2010) 172-176.
- [28] H. A. Chapman. Endosomal proteases in antigen presentation. *Curr Opin*

Immunol 18 (2006) 78-84.

- [29] C. Juliana, T. Fernandes-Alnemri, J. Wu, P. Datta, L. Solorzano, J. W. Yu, R. Meng, A. A. Quong, E. Latz, C. P. Scott, E. S. Alnemri. Anti-inflammatory compounds parthenolide and Bay 11-7082 are direct inhibitors of the inflammasome. *J Biol Chem* 285 (2010) 9792-9802.
- [30] H. Zhang, C. Zhong, L. Shi, Y. Guo, Z. Fan. Granulysin induces cathepsin B release from lysosomes of target tumor cells to attack mitochondria through processing of bid leading to Necroptosis. *J Immunol* 182 (2009) 6993-7000.
- [31] K. Niikura, S. Sekiguchi, T. Nishio, T. Masuda, H. Akita, Y. Matsuo, K. Kogure, H. Harashima, K. Ijiro. Oligosaccharide-mediated nuclear transport of nanoparticles. *ChemBiochem* 9 (2008) 2623-2627.
- [32] S. A. Adam, R. S. Marr, L. Gerace. Nuclear protein import in permeabilized mammalian cells requires soluble cytoplasmic factors. *J Cell Biol* 111 (1990) 807-816.
- [33] T. Naka, M. Narazaki, M. Hirata, T. Matsumoto, S. Minamoto, A. Aono, N. Nishimoto, T. Kajita, T. Taga, K. Yoshizaki, S. Akira, T. Kishimoto. Structure and function of a new STAT-induced STAT inhibitor. *Nature* 387 (1997) 924-929.
- [34] A. Yoshimura, T. Naka, M. Kubo. SOCS proteins, cytokine signalling and immune regulation. *Nat Rev Immunol* 7 (2007) 454-465.

Figure legends

Fig. 1. Construction and functional analysis of the YSK12-MEND. (a) Chemical structural formula of YSK12-C4. (b) Conceptual image of YSK12-MEND. YSK12-MEND was composed of YSK12-C4, cholesterol and PEG-DMG (85/15/1 molar ratio). (c) TEM image of the YSK12-MEND. (d) Dose response curve for gene silencing efficiency against the SR-B1 gene in BMDCs. BMDCs were treated with the YSK12-MEND, RNAiMAX or R8/GALA-MEND_{SUV} and the mRNA levels of SR-B1 were measured by quantitative RT-PCR at 24 h after the treatment. The vertical axis shows the relative SR-B1/GAPDH mRNA level, in which the mean value of the no treatment BMDCs was assumed to be 1.0. Data are the mean \pm SEM (n=3-5). (e) Cell viability of BMDCs. BMDCs were treated with YSK12-MEND, RNAiMAX or R8/GALA-MEND_{SUV} (siRNA doses of 3, 10, 100 nM) and the cell viability was measured at 2 h after the treatment. Data are the mean \pm SEM (n=3).

Fig. 2. Quantitative analysis of cellular uptake of the YSK12-MEND. BMDCs were treated with DiI-labeled the YSK12-MEND, RNAiMAX or R8/GALA-MEND_{SUV}. The fluorescence intensity in the cells was measured at 30 min after the treatment. Data are the mean \pm SEM (**P<0.01, n=3).

Fig. 3. Analysis of membrane disruption activity of the YSK12-MEND. (a) Hemolysis assay. RBC suspension was mixed with YSK12-MEND, RNAiMAX or R8/GALA-MEND_{SUV} at final siRNA concentrations of 0, 60, 120, 240 nM and the mixtures were incubated for 30 min at 37°C. The absorbance due to hemoglobin was measured. Data are the mean \pm SEM (n=3). (b) Scheme of analysis of cathepsin B release to the cytosol. (c) Analysis of cathepsin B activity in the cytosol. BMDCs were treated with YSK12-MEND, RNAiMAX or R8/GALA-MEND_{SUV} at siRNA doses of 10, 30 and 100 nM and the activity of cathepsin B released to the cytosol was measured at 2 h after the treatment. Data are the mean \pm SEM (**P<0.01, n=3).

Fig. 4. Analysis of immune responses in SOCS1-silenced BMDCs by the YSK12-MEND. BMDCs were treated with YSK12-MEND, RNAiMAX or R8/GALA-MEND_{SUV}. The anti-SOCS1 siRNA doses were 3, 10 and 30 nM. The control siRNA (anti-human PLK1 siRNA) dose was 30 nM. (a) Gene silencing against SOCS1 in BMDCs. The mRNA levels of SOCS1 were measured by quantitative RT-PCR at 30 h after the treatment. The vertical axis shows the relative

SOCS1/GAPDH mRNA level, in which the mean value of the no treatment BMDCs was assumed to be 1.0. Data are the mean \pm SEM (**P<0.01, *P<0.05, n=3). The concentration of TNF- α (b) and IL-6 (c) in the supernatant at 30 h after the treatment was measured by ELISA. Data are the mean \pm SEM (**P<0.01 v.s. vehicle, n=3).

Fig. 5. Antitumor effect mediated by SOCS1-silenced BMDCs by the YSK12-MEND. (a) Preventative antitumor effect. Mice were immunized with BMDCs treated with the YSK12-MEND, RNAiMAX or R8/GALA-MEND_{SUV}. The dose of anti-SOCS1 siRNA and control siRNA (anti-human PLK1 siRNA) was 30 nM. At 7 days after the immunization, E.G7-OVA cells were inoculated to the immunized mice and tumor growth was monitored. Data are the mean \pm SEM (**P<0.01, *P<0.05, n=3-5). (b) Therapeutic antitumor effect. Mice were inoculated with E.G7-OVA cells. On days 4, 7 and 15, the mice were immunized with BMDCs treated with the YSK12-MEND or RNAiMAX and the tumor growth was monitored. The dose of anti-SOCS1 siRNA and control siRNA (anti-human PLK1 siRNA) was 30 nM. Data are the mean \pm SEM (**P<0.01, *P<0.05, n=5).